ICIC Express Letters
Volume **11**, Number **7**, July **2017**

ICIC International ©2017 ISSN 1881-803X
pp. 1191–1198

AN AZIMUTH-ELEVATION ESTIMATION ALGORITHM FOR VECTOR SENSOR ARRAY BASED ON RANK-$(L_1, L_2, \cdot)$ BCD

Yufei Gao[1], Guan Gui[2], Wei Xie[1], Yanbin Zou[1], Yue Yang[1] and Qun Wan[1]

[1]School of Electronic Engineering
University of Electronic Science and Technology of China
No. 2006, Xiyuan Ave., West Hi-Tech Zone, Chengdu 611731, P. R. China
wanqun@uestc.edu.cn

[2]College of Telecommunication and Information Engineering
Nanjing University of Posts and Telecommunications
No. 66, Xinmofan Road, Nanjing 210003, P. R. China
guiguan@njupt.edu.cn

Received January 2017; accepted April 2017

Abstract. *An azimuth-elevation two-dimensional angle of arrival (2-D AOA) estimation algorithm for the L-shaped electromagnetic vector sensor (EMVS) array is presented in this paper. This algorithm is based on the rank-$(L_1, L_2, \cdot)$ block component decomposition (BCD) tensor modeling, which can make the most of the multiway structural information of electromagnetic signals accomplish the blind estimation of array parameters. Besides, the algorithm can automatically achieve the azimuth and elevation angles pair-matching of the partially polarized signal. The numerical experiment results demonstrate that even under the conditions of low SNR and small angular separations, the proposed algorithm still maintains the advantage on accuracy and robustness of parameter estimation.*

Keywords: EMVS array, 2-D AOA, Partially polarized signal, Tensor decomposition, Rank-$(L_1, L_2, \cdot)$ BCD

1. **Introduction.** Different from the traditional scalar sensor, electromagnetic vector sensor (EMVS) can detect electromagnetic wave with different polarization forms and fully acquire information carried by the wave. Many algorithms have been presented to study the problem of parameter estimation of EMVS array, including MUSIC [1], ESPRIT [2] and other methods [3, 4, 5, 6, 7]. However, the existing methods are based on either one-dimensional vector or two-dimensional matrix modeling, which are inappropriate to the received signal of EMVS array with inherent multiway structure. In recent years, the tensor-based method has become a research hotspot in signal processing [8, 9]. Compared with vector and matrix modeling, tensor modeling is more suitable to the multiway structure signal [10, 11]. For this reason, tensor decomposition has been applied in EMVS array signal processing in the past decade [1, 12, 13, 14, 15]. However, the existing tensor-decomposition-based parameter estimation methods for EMVS array are mostly based on canonical polyadic decomposition (CPD) modeling. Such model has the advantage of decomposition uniqueness, whereas the decomposition factors must be rank-1, which may not be satisfied in practice [16]. It is expected that a new framework needs to be developed, which not only can maintain the uniqueness of decomposition but also relax the requirement for rank constraint. In 2008, L. De Lathauwer proposed a tensor decomposition model, i.e., block component decomposition (BCD), which is able to overcome such defect [17, 18]. BCD-based methods maintain the advantages of the existing tensor decomposition methods and have various forms [19, 20, 21, 22]. To the best of our knowledge, few papers report the application of BCD for vector sensor array. Besides, the angle pair-matching is a difficult problem for 2-D AOA of array signal

processing. Since BCD method possesses the blind estimation feature, it can solve such problem suitably. Motivated by the background above, this paper proposes a BCD-based parameter estimation algorithm for the EMVS array.

The rest of this paper is organized as follows. Section 2 describes the received signal model of EMVS array based on BCD modeling; Section 3 develops the algorithm based on rank-$(L_1, L_2, \cdot)$ BCD for 2-D AOA estimation; Section 4 presents numerical simulations to verify the proposed algorithm; the last section concludes this paper.

2. **BCD Modeling for EMVS Array.** Consider an L-shaped EMVS array, as shown in Figure 1, which consists of a couple of orthogonal uniform linear arrays and each has M sensors. For partially polarized electromagnetic waves [3, 4], the received signal model can be expressed as

$$\boldsymbol{x}(t) = (\boldsymbol{A}_x \odot \boldsymbol{\Psi})\, \boldsymbol{s}^T(t) + \boldsymbol{n}_x(t), \tag{1}$$

$$\boldsymbol{z}(t) = (\boldsymbol{A}_z \odot \boldsymbol{\Psi})\, \boldsymbol{s}^T(t) + \boldsymbol{n}_z(t), \tag{2}$$

where the operator $\odot$ denotes the Khatri-Rao product with block form [17]; the source signal is $\boldsymbol{s}(t) = \left[\tilde{s}_1^{(1)}(t), \tilde{s}_2^{(1)}(t), \ldots, \tilde{s}_1^{(K)}(t), \tilde{s}_2^{(K)}(t)\right] \in \mathbb{C}^{1\times 2K}$, where $\left(\tilde{s}_1^{(k)}(t), \tilde{s}_2^{(k)}(t)\right)$ denotes the k-th signal complex envelope; $\boldsymbol{n}_x(t) \in \mathbb{C}^{M\times 1}$ is the additive white Gaussian noise (AWGN) vector; $\boldsymbol{A}_x = [\boldsymbol{a}_{x,1}, \boldsymbol{a}_{x,2}, \ldots, \boldsymbol{a}_{x,K}] \in \mathbb{C}^{M\times K}$ is the steering matrix of the subarray along x-axis. Let d denote the array element spatial interval and define the spatial frequency $\alpha_k = -\frac{2\pi d}{\lambda}\cos\phi_k'$, in which λ is the wavelength of source signal; then we have $\boldsymbol{a}_{x,k} = \left[1, e^{j\alpha_1}, e^{j\alpha_2}, \cdots, e^{j(M-1)\alpha_K}\right]^T$. $\boldsymbol{\Psi} = [\boldsymbol{\Theta}_1, \ldots, \boldsymbol{\Theta}_K]$, where $\boldsymbol{\Theta}_k \in \mathbb{R}^{6\times 2}$ is the polarization parameter matrix. The signal model of the subarray along z-axis has the same form as that along x-axis. Without loss of generality, the argument t is omitted in the following discussions for simplicity.

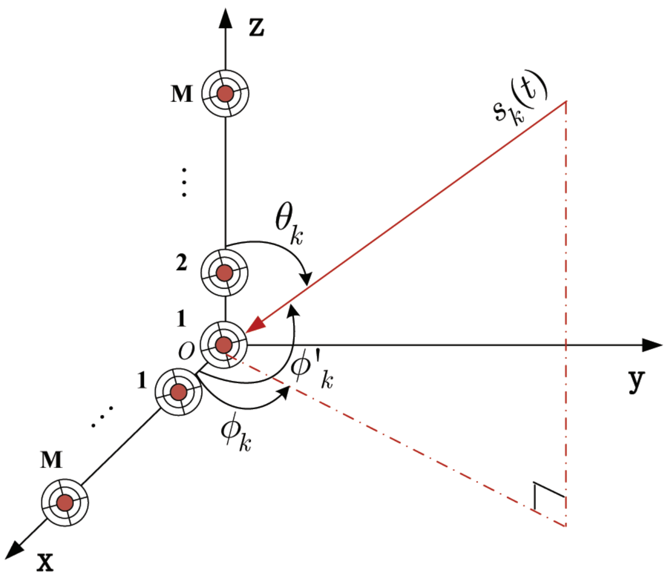

FIGURE 1. L-shaped array configuration of EMVS array

Merge measurement with the both subarrays [4], and then received signal model can be expressed as

$$\boldsymbol{y} = \sum_{k=1}^{K} \boldsymbol{A}_k \otimes \boldsymbol{\Theta}_k \boldsymbol{s}_k^T + \boldsymbol{n}, \tag{3}$$

where $\otimes$ denotes the Kronecker product. The corresponding matrix form is

$$\boldsymbol{Y} = (\boldsymbol{A} \odot \boldsymbol{\Psi})\, \boldsymbol{S}^T + \boldsymbol{N}, \tag{4}$$

in which $\boldsymbol{A} = [\boldsymbol{A}_1, \ldots, \boldsymbol{A}_K]$ with $\boldsymbol{A}_k = blockdiag\,(\boldsymbol{a}_{x,k}, \boldsymbol{a}_{z,k})$, where $blockdiag\,(\cdot)$ denotes a block diagonal matrix; $\boldsymbol{S} = \left[\boldsymbol{S}_1^T, \ldots, \boldsymbol{S}_K^T\right]$ with $\boldsymbol{S}_k = \left[\boldsymbol{s}_k\,(1)^T, \ldots, \boldsymbol{s}_k\,(N)^T\right]$; $\boldsymbol{N}$ is the corresponding AWGN matrix. Note that (4) is a rank-$(L_1, L_2, \cdot)$ BCD model [17], where $L_1 = L_2 = 2$. In this paper, the calligraphic capital letter is utilized to denote the tensor data, and then the received signal model can be rewritten as

$$\mathcal{Y} = \sum_{k=1}^{K} \mathcal{S}_k \times_1 \boldsymbol{A}_k \times_2 \boldsymbol{\Theta}_k + \mathcal{N}, \tag{5}$$

where $\times_n$ denotes the mode-n product between tensor and matrix, in which *mode* is considered as the order of tensor data [8]. $\mathcal{S}_k \in \mathbb{C}^{L_1 \times L_2 \times N}$ is the k-th source signal, of which the mode-3 matricization is $\boldsymbol{S}_k^T$, i.e., $\boldsymbol{S}_k^T = [\mathcal{S}_k]_{(3)}$.

Next, we investigate whether the rank condition of each factor is satisfied in (5). Note that the steering matrix $\{\boldsymbol{A}_k\}_{k=1}^K \in \mathbb{C}^{ML_1 \times L_1}$ is of full column rank when $M \geq 1$. The same is true for $\{\boldsymbol{\Theta}_k\}_{k=1}^K \in \mathbb{R}^{6 \times L_2}$ when $L_2 < 6$. Define the mode-n rank of a tensor as the rank of its mode-n matricization [9]. For $\{\mathcal{S}_k\}_{k=1}^K \in \mathbb{C}^{L_1 \times L_2 \times N}$, the size of mode-1 matricization is $(L_1 \times NL_2)$ and $(L_2 \times NL_1)$ for mode-2. Thus the mode-1 and mode-2 rank of $\{\mathcal{S}_k\}_{k=1}^K$ are L_1 and L_2, respectively, when snapshots N is sufficiently large. Consequently, the rank condition of each factor in (5) can be satisfied if

$$\begin{cases} M \geq 1, \\ L_2 \leq 6, \\ N \geq \max\left(\left\lceil \frac{L_1}{L_2} \right\rceil, \left\lceil \frac{L_2}{L_1} \right\rceil\right). \end{cases} \tag{6}$$

For the L-shaped array in this paper, on each subarray the number of sensors $M > 1$ must be true. And since $L_1 = L_2 = 2$, for either single or multiple snapshots, Equation (5) will be valid according to (6).

3. AOA Estimation Algorithm.

Given the rank-$(L_1, L_2, \cdot)$ BCD model (5) with additive noise, the proposed algorithm is to acquire the estimation of factor matrices $\{\boldsymbol{A}_k\}_{k=1}^K$, $\{\boldsymbol{\Theta}_k\}_{k=1}^K$ from the received signal $\mathcal{Y}$ and obtain the estimation of spatial frequency $\{\alpha_k\}_{k=1}^K$. This paper adopts the minimum mean square error (MMSE) criterion [18],

$$\begin{aligned} &\min_{\hat{\boldsymbol{A}}_k, \hat{\boldsymbol{\Theta}}_k} \left\| \mathcal{Y} - \hat{\mathcal{Y}} \right\|_F^2, \quad k = 1, 2, \ldots, K, \\ &\text{s.t.} \quad \hat{\mathcal{Y}} = \sum_{k=1}^{K} \hat{\mathcal{S}}_k \times_1 \hat{\boldsymbol{A}}_k \times_2 \hat{\boldsymbol{\Theta}}_k, \end{aligned} \tag{7}$$

where $\|\cdot\|_F$ denotes the Frobenius norm. Several algorithms can be employed to solve the above problems [18, 23, 24]. The typical one is alternating least squares (ALS) [8, 24]. With fixed two components of $\boldsymbol{A}, \boldsymbol{\Psi}, \boldsymbol{S}$ in each iteration, the remaining one is updated by least squares approach, and then the same scheme is repeated in turn until the convergence condition is satisfied.

For the array manifold configuration in this paper, $\boldsymbol{A}_k$ can be parted as $\boldsymbol{A}_k = \left[\boldsymbol{A}_{k,1}^T, \boldsymbol{A}_{k,2}^T\right]^T$, where $\boldsymbol{A}_{k,1} = [\boldsymbol{a}_{x,k}, \boldsymbol{0}]$, $\boldsymbol{A}_{k,2} = [\boldsymbol{0}, \boldsymbol{a}_{z,k}]$. Because the BCD estimation result and steering matrix have the same column space [17], $\hat{\boldsymbol{A}}_k$ is parted as $\hat{\boldsymbol{A}}_k = \left[\hat{\boldsymbol{A}}_{k,1}^T, \hat{\boldsymbol{A}}_{k,2}^T\right]^T$ in the same way. Then we have

$$\hat{\boldsymbol{A}}_{k,1} = [\boldsymbol{a}_{x,k}, \boldsymbol{a}_{x,k}] \cdot diag\left([\boldsymbol{\Gamma}_k]_{1,:}\right), \tag{8}$$

$$\hat{\boldsymbol{A}}_{k,2} = [\boldsymbol{a}_{z,k}, \boldsymbol{a}_{z,k}] \cdot diag\left([\boldsymbol{\Gamma}_k]_{2,:}\right). \tag{9}$$

The above equations indicate that $\hat{\boldsymbol{A}}_{k,m}$ is a rank-1 matrix and has the same column space as the steering vector. Hence the spacial frequency can be estimated by subspace methods. Giving the singular value decomposition (SVD) of $\hat{\boldsymbol{A}}_{k,m}$,

$$\hat{\boldsymbol{A}}_{k,m} = \boldsymbol{U}_{k,m}\boldsymbol{\Sigma}_{k,m}\boldsymbol{V}_{k,m}^H,\ m = 1, 2, \tag{10}$$

the left singular vector $\boldsymbol{u}_{k,1}$ corresponding to the maximum singular value can be obtained. Take the first and last $(M-1)$ rows of $\boldsymbol{u}_{k,1}$, denoted as $\boldsymbol{u}_a$ and $\boldsymbol{u}_b$, to construct $\boldsymbol{U}_{ab} = [\boldsymbol{u}_a, \boldsymbol{u}_b]$. Applying eigen value decomposition of $\boldsymbol{U}_{ab}^H\boldsymbol{U}_{ab}$, i.e., $\boldsymbol{U}_{ab}^H\boldsymbol{U}_{ab} = \boldsymbol{W}\boldsymbol{\Lambda}\boldsymbol{W}^H$, where

$$\boldsymbol{W} = \begin{bmatrix} w_{1,1} & w_{1,2} \\ w_{2,1} & w_{2,2} \end{bmatrix} \in \mathbb{C}^{2\times 2}, \tag{11}$$

yields the estimation of spacial frequency $\hat{\alpha}_k = \angle\left(-\frac{w_{1,2}}{w_{2,2}}\right)$, where $\angle(\cdot)$ denotes the phase angle of a complex variable. Thus the estimation of the arrival angle on the array along x-axis can be obtained, $\hat{\phi}'_k = \arccos\left(\frac{-\hat{\alpha}_k\lambda}{2\pi d}\right)$. The same method can be used to get the estimation of the elevation angle $\hat{\theta}_k$. After obtaining the estimation of ϕ'_k and θ_k, the azimuth angle ϕ_k can be estimated directly, $\hat{\phi}_k = \arccos\left(\frac{\cos\hat{\phi}'_k}{\sin\hat{\theta}_k}\right)$.

Since $\hat{\boldsymbol{A}}_k$ includes the steering vector information on both subarrays and the type-2 BCD possesses the uniqueness [17, 18], the estimation of azimuth and elevation angles accomplish the matching pairing automatically. It should be noted that even if the array manifold is arbitrarily configured and no longer has the Vandermonde structure, the spacial frequency can still be estimated by utilizing the one dimensional spectral peak search method.

4. Numerical Simulations and Discussion.

4.1. Realization of 2-D AOA estimation.

In this section, two simulation experiments are demonstrated for proving the validation of the proposed method, as shown in Figure 2. The experimental scenario is consistent with the received signal model (5). The number of sensors in the subarray is assumed as $M = 5$; the number of source signals $K = 2$; the number of snapshots $N = 200$. The Monte-Carlo independent trials is $L = 500$.

In the first experiment, two groups of the AOAs are $(\phi_1, \theta_1) = (100°, 65°)$ and $(\phi_2, \theta_2) = (120°, 45°)$; the SNR range is -3dB $\sim$ 15dB. The result indicates that the proposed algorithm has the good estimation accuracy even if the SNR is low, as shown in Figure 2(a). In the second experiment, the SNR is fixed at 5dB and two groups of AOA are selected as $(\phi_1, \theta_1) = (100°, 65°)$, $(\phi_2, \theta_2) = (\phi_1 + \Delta, \theta_1 + \Delta)$, where $\Delta \in [1°, 20°]$ denotes the angular separation. As shown in Figure 2(b), the AOA estimation can be fully distinguished when the angular separation is larger than 3°. Even if the separation degree is very small, the paired angles can still be estimated correctly with a high probability.

4.2. Performance comparison.

The comparison of the proposed algorithm with three existing methods has been investigated in this section, which shows the performance in both root mean square error (RMSE) and detection probability. The reference methods include classic subspace methods, i.e., MUSIC [1], ESPRIT [2], and the CPD-based 2-D AOA estimation method [11]. The parameter settings are the same as those in Section 4.1.

4.2.1. *RMSE.* First, we investigate the RMSE which is defined as $\sqrt{\frac{1}{L}\sum_{l=1}^{L}(\epsilon_\phi(l)^2 + \epsilon_\theta(l)^2)}$, where $\epsilon_\phi(l) = \frac{1}{K}\sum_{k=1}^{K}\left|\hat{\phi}_k(l) - \phi_k\right|$, $\epsilon_\theta(l) = \frac{1}{K}\sum_{k=1}^{K}\left|\hat{\theta}_k(l) - \theta_k\right|$, in which $\left(\hat{\phi}_k(l), \hat{\theta}_k(l)\right)$ are the estimation values of k-th azimuth-elevation angles for l-th Monte-Carlo trial. The Cramer-Rao lower bound is defined as $\sqrt{\frac{1}{K}\sum_{k=1}^{K}\left(CRB\left(\phi_k\right) + CRB\left(\theta_k\right)\right)}$, where

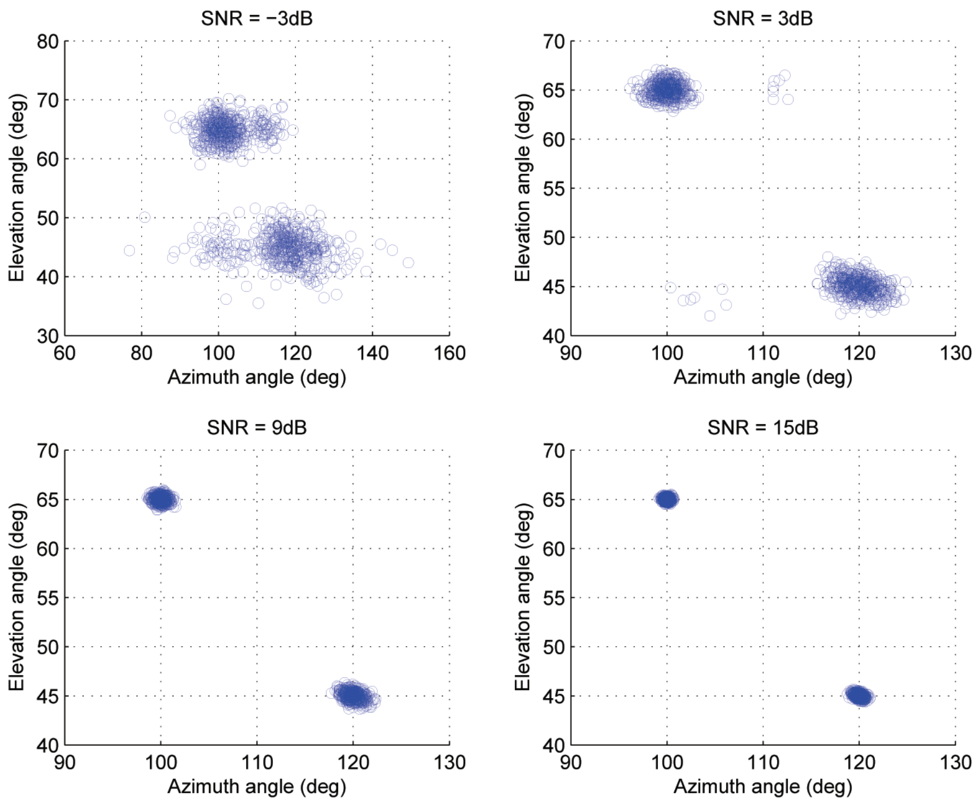

(a) Under different SNRs

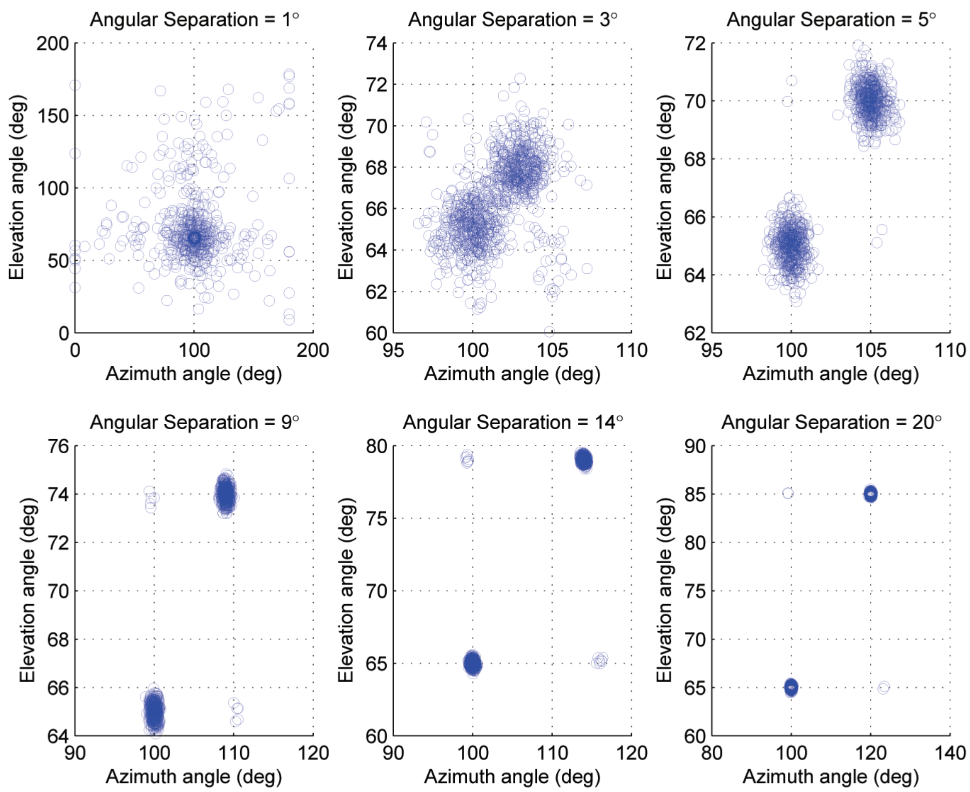

(b) Under different angular separations

FIGURE 2. Azimuth-elevation scatterplots, by 500 Monte-Carlo trials ($M = 5, K = 2, N = 200$)

$CRB(\phi_k)$ and $CRB(\theta_k)$ are the diagonal elements of CRB matrix [3], corresponding to the parameters ϕ_k and θ_k, respectively.

The RMSE curves versus SNRs and angular separations are shown in Figure 3. Of all the methods, the RMSE of the proposed algorithm is the lowest for the whole range of SNR and angular separation according to the results. The two tensor-decomposition-based algorithms are better than those matrix-based subspace algorithms, since tensor decomposition algorithm can make the best of the multiway structure information in received signal. As the analysis in Section 3, the BCD algorithm can obtain the steering matrix $\boldsymbol{A}_k$ directly, and then automatically achieve the matching pair of the azimuth and elevation angles. Therefore, the detection probability of BCD is higher than CPD. The results in Section 4.2.2 provide the similar conclusion. It is noted that RMSE curves vary with the steeper slope as the separation degree less than 5°, which reveals the sensitivity to angular separation within such interval. Even under the demanding conditions, the proposed algorithm has the better performance.

4.2.2. *Detection probability.* The detection probability measures the success rate of pair-matching for two groups of azimuth-elevation angles. In this section, detection probabilities of the four methods are compared in accordance with two simulation experiments, as shown in Figure 4. The results show that the proposed algorithm maintains the highest success rate of pair-matching under the conditions of low SNR and small angular

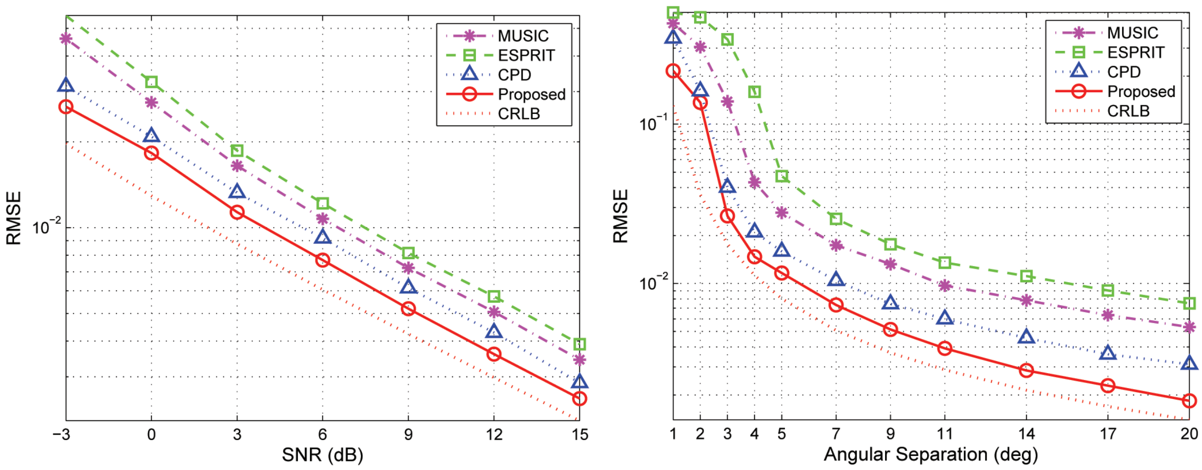

FIGURE 3. RMSE versus SNRs and angular separations, by 500 Monte-Carlo trials ($M = 5, K = 2, N = 200$)

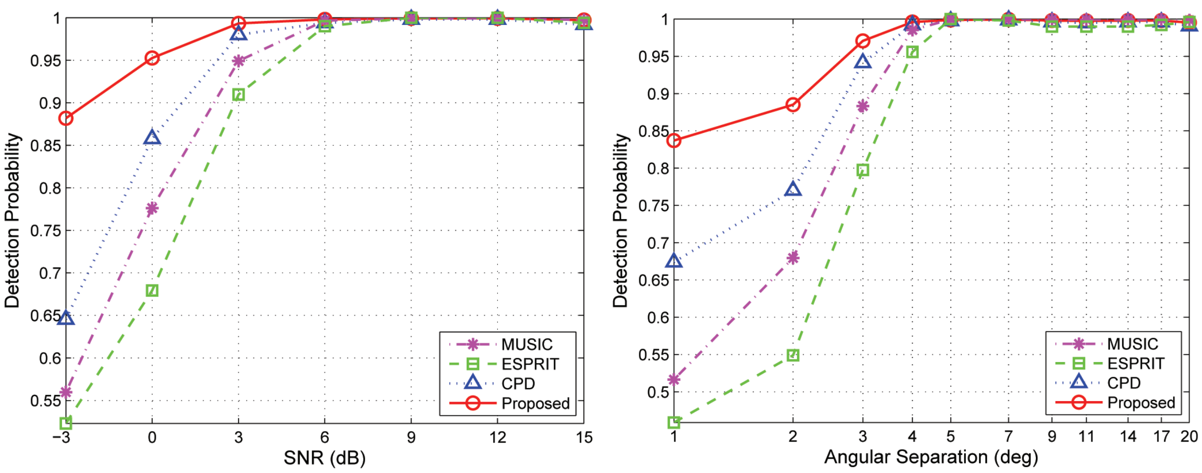

FIGURE 4. Detection probability versus SNRs and angular separations, by 500 Monte-Carlo trials ($M = 5, K = 2, N = 200$)

separations. For example, when SNR = −3dB, the detection probability of the proposed algorithm reaches to 88%, increased by 69%, 57% and 35% compared with ESPRIT (52%), MUSIC (56%) and CPD (65%), respectively. When the angular separation $\Delta = 1^\circ$, the success rate of proposed algorithm is 84%, increased by about 83%, 61% and 25% compared with ESPRIT (46%), MUSIC (52%) and CPD (67%), respectively. This benefit by automatic angles pairing resulted from the estimating steering vectors and the decomposition uniqueness of BCD, which makes the proposed algorithm obtain the better detection ability and achieve the best estimation performance under the severe environment.

5. **Conclusion.** This paper investigates the BCD tensor modeling in parameter estimation of EMVS array. For the partially polarized signal, a rank-$(L_1, L_2, \cdot)$ BCD-based algorithm is developed to achieve the 2-D AOA estimation. This algorithm can fully make use of the multiway structural information of the received signal and automatically obtain the paired azimuth and elevation angles. Several numerical experiments are carried out to verify the effectiveness of the algorithm. The experiment results show that both the estimation accuracy and detection probability of this algorithm are superior to the subspace methods based on matrix decomposition and CPD method based on tensor decomposition. The proposed algorithm manifests robust and good performance under severe conditions such as low SNR and small angular separations. The future work is to study the case of coherent signals, which is common in the practical application.

Acknowledgment. This work is partially supported by the National Natural Science Foundation of China under Grant U1533125, National Science and Technology Major Project under Grant 2016ZX03001022, and the Fundamental Research Funds for the Central Universities under Grant ZYGX2015Z011.

REFERENCES

[1] X. Gong, Z. Liu, Y. Xu and M. I. Ahmad, Direction-of-arrival estimation via twofold mode-projection, *Signal Processing*, vol.89, no.5, pp.831-842, 2009.
[2] K. T. Wong and M. D. Zoltowski, Uni-vector-sensor ESPRIT for multisource azimuth, elevation, and polarization estimation, *IEEE Trans. Antennas and Propagation*, vol.45, no.10, pp.1467-1474, 1997.
[3] A. Nehorai and E. Paldi, Vector-sensor array processing for electromagnetic source localization, *IEEE Trans. Signal Processing*, vol.42, no.2, pp.376-398, 1994.
[4] K.-C. Tan, K.-C. Ho and A. Nehorai, Linear independence of steering vectors of an electromagnetic vector sensor, *IEEE Trans. Signal Processing*, vol.44, no.12, pp.3099-3107, 1996.
[5] K. T. Wong and M. D. Zoltowski, Closed-form direction finding and polarization estimation with arbitrarily spaced electromagnetic vector-sensors at unknown locations, *IEEE Trans. Antennas and Propagation*, vol.48, no.5, pp.671-681, 2000.
[6] X. Yuan, Estimating the DOA and the polarization of a polynomial-phase signal using a single polarized vector-sensor, *IEEE Trans. Signal Processing*, vol.60, no.3, pp.1270-1282, 2012.
[7] H. K. Xiao, L. Zou, B. G. Xu, S. L. Tang, Y. H. Wan, Y. L. Liu and Q. Wan, Direction and polarization estimation with modified quad-quaternion music for vector sensor arrays, *The 12th International Conference on Signal Processing (ICSP)*, pp.352-357, 2014.
[8] T. G. Kolda and B. W. Bader, Tensor decompositions and applications, *SIAM Review*, vol.51, no.3, pp.455-500, 2009.
[9] A. Cichocki, D. Mandic, L. De Lathauwer, G. Zhou, Q. Zhao, C. Caiafa and H. A. Phan, Tensor decompositions for signal processing applications: From two-way to multiway component analysis, *IEEE Signal Processing Magazine*, vol.32, no.2, pp.145-163, 2015.
[10] N. D. Sidiropoulos, R. Bro and G. B. Giannakis, Parallel factor analysis in sensor array processing, *IEEE Trans. Signal Processing*, vol.48, no.8, pp.2377-2388, 2000.
[11] Y.-F. Gao, Y.-H. Wan, S.-L. Tang, B.-G. Xu and Q. Wan, A CPD-based AOA estimation algorithm with vandermonde-constrained preprocessing approach, *The 10th International Conference on Information, Communications and Signal Processing (ICICS)*, pp.1-5, 2015.
[12] S. Miron, N. Le Bihan and J. I. Mars, Vector-sensor music for polarized seismic sources localization, *EURASIP Journal on Advances in Signal Processing*, vol.2005, no.1, pp.1-11, 2005.

[13] X. Guo, S. Miron, D. Brie, S. Zhu and X. Liao, A candecomp/parafac perspective on uniqueness of doa estimation using a vector sensor array, *IEEE Trans. Signal Processing*, vol.59, no.7, pp.3475-3481, 2011.

[14] K. Han and A. Nehorai, Nested vector-sensor array processing via tensor modeling, *IEEE Trans. Signal Processing*, vol.62, no.10, pp.2542-2553, 2014.

[15] P. Forster, G. Ginolhac and M. Boizard, Derivation of the theoretical performance of a tensor music algorithm, *Signal Processing*, 2016.

[16] A. Stegeman, Candecomp/parafac: From diverging components to a decomposition in block terms, *Siam Journal on Matrix Analysis and Applications*, vol.33, no.2, pp.209-215, 2012.

[17] L. De Lathauwer, Decompositions of a higher-order tensor in block terms – Part II: Definitions and uniqueness, *SIAM Journal on Matrix Analysis and Applications*, vol.30, no.3, pp.1033-1066, 2008.

[18] L. De Lathauwer and D. Nion, Decompositions of a higher-order tensor in block terms – Part III: Alternating least squares algorithms, *SIAM journal on Matrix Analysis and Applications*, vol.30, no.3, pp.1067-1083, 2008.

[19] D. Nion and L. De Lathauwer, A block component model-based blind DS-CDMA receiver, *IEEE Trans. Signal Processing*, vol.56, no.11, pp.5567-5579, 2008.

[20] L. De Lathauwer, Blind separation of exponential polynomials and the decomposition of a tensor in rank-$(l_r, l_r, 1)$ terms, *SIAM Journal on Matrix Analysis and Applications*, vol.32, no.4, pp.1451-1474, 2011.

[21] Q. Zhao, C. F. Caiafa, D. P. Mandic, Z. C. Chao, Y. Nagasaka, N. Fujii, L. Zhang and A. Cichocki, Higher order partial least squares (HOPLS): A generalized multilinear regression method, *IEEE Trans. Pattern Analysis and Machine Intelligence*, vol.35, no.7, pp.1660-1673, 2013.

[22] P. Tichavsky, A. H. Phan and A. Cichocki, Non-orthogonal tensor diagonalization, a tool for block tensor decompositions, *Computer Science*, 2015.

[23] D. Nion and L. De Lathauwer, An enhanced line search scheme for complex-valued tensor decompositions. application in DS-CDMA, *Signal Processing*, vol.88, no.3, pp.749-755, 2008.

[24] L. Sorber, M. Van Barel and L. De Lathauwer, Optimization-based algorithms for tensor decompositions: Canonical polyadic decomposition, decomposition in rank-$(l_r, l_r, 1)$ terms, and a new generalization, *SIAM Journal on Optimization*, vol.23, no.2, pp.695-720, 2013.